ISTITUTO NAZIONALE DI FISICA NUCLEARE

Sezione di Trieste

INFN/BE-92/04

22 luglio 1992

D. Chatellard, F. Ciocci, G. Dattoli, P. De Cecco, F. Della Valle,M. Denoréaz, A. Doria, J.-P. Egger, G.P. Gallerano, L. Giannessi, G. Giubileo, P. Hauser, E. Jeannet, F. Kottmann, G. Messina, E. Milotti, C. Petitjean, A. Renieri, C. Rizzo, L.M. Simons, D. Taqqu, A. Vacchi, A. Vignati and E. Zavattini

LASER SPECTROSCOPY OF MUONIC HYDROGEN

Servizio Documentazione
dei Laboratori Nazionali di Frascati

LASER SPECTROSCOPY OF MUONIC HYDROGEN

F. DELLA VALLE, E. MILOTTI, C. RIZZO, A. VACCHI, E. ZAVATTINI
Dipartimento di Fisica dell'Università di Trieste
and
Istituto Nazionale di Fisica Nucleare,
Sezione di Trieste, Via Valerio 2, I-34127 Trieste, Italy

D. CHATELLARD, M. DENORÉAZ, J.-P.EGGER, E. JEANNET
Institut de Physique de l'Université,
Breguet 1, CH-2000, Neuchâtel, Switzerland

F. CIOCCI, G. DATTOLI, A. DORIA, G.P. GALLERANO, L. GIANNESSI,
G. GIUBILEO, G. MESSINA, A. RENIERI, A. VIGNATI
ENEA - Area INN, Dipartimento Sviluppo Tecnologie di Punta,
Centro Ricerche Energia, I-00044 Frascati, Italy

P. DE CECCO, P. HAUSER, F. KOTTMANN, C. PETITJEAN,
L.M. SIMONS, D. TAQQU,
Paul Scherrer Institut,
CH-5232 Villigen PSI, Switzerland

Presented by E. Zavattini at the
"Workshop on Muonic Atoms and Molecules"
April 1992, Ascona (Switzerland)

Abstract.

We present here a discussion about the physics motivations and the experimental feasibility of our recent experimental proposal "Spectroscopy of Muonic Hydrogen" presented to the Dec. 1991 meeting of the PSI Benutzervesammlung (proposal R-9206-1).

1. Introduction.

In this paper we describe an experimental plan to measure, with high accuracy, the energy differences between levels with principal quantum number $n \leq 4$ of muonic hydrogen (μp). The experimental method is to irradiate the excited muonic atom, during its formation, with an intense, tuneable laser radiation, and detect at the same time the K_α and K_β X-rays emitted by the excited $(\mu p)^*$ system as it cascades electromagnetically toward the ground level. When the frequency of the laser radiation has the correct value to excite a transition between two of the levels involved in the cascade the intensities of some of the K lines will change. By detecting these intensity changes, while tuning the laser, we will be able to measure the energy difference between the two levels with great precision [1].

To perform such an experiment we need

1. A proper low-energy μ^--beam. Each incoming muon, which may either decay in flight or stop in the target, must be tagged by a proper scintillator counter approximately $1 \div 2$ μsec before it stops in the hydrogen gas target to trigger in advance the necessarily intense electromagnetic radiation source.

2. A special cavity-target, containing in the stopping region a proper infrared cavity, where the hydrogen gas is at a rather low pressure. To reduce the interaction rate of collision of the $(\mu p)^*$ atom with the neighbouring hydrogen molecules H_2, the pressure must be kept around or below 30 mbar [2]. Moreover the spatial distribution of the stopped muons in the target must have sufficiently small dimensions so that we can achieve a high electromagnetic energy density in the stopping region.

3. A pulsed tuneable far-infrared source of high and stable intensity with a relative linewidth $\leq 0.5\%$.

4. High-resolution X-ray detectors: these detectors must be able to distinguish the K_α, K_β and K_γ lines of the (μp) system.

In what follows we wish to discuss first the physics motivations for such a program; then we will discuss its experimental feasibility.

2. Theoretical overview.

The energy levels of the muonic hydrogen atom can be computed within the framework of the Dirac theory: the hyperfine corrections, recoil corrections, etc., can be introduced as usual. To agree with the experimental results, one has to include also the Quantum Electrodynamics radiative corrections.

Thus the list of physics motivations in the field of muonic hydrogen spectroscopy includes the following items:

i) Test of the QED radiative corrections in a lepton-hadron bound system [1,3].

The QED radiative corrections, to the lowest order, can be classified in two broad categories: the vertex corrections and the photon propagator corrections. The first are associated to the quantum fluctuations of the electromagnetic field, whereas the second, called QED vacuum polarization corrections, are associated with the quantum fluctuations of the electron-positron field.

In general for a muonic atom the QED vertex corrections are extremely small compared to the QED vacuum polarization corrections [3].

The muonic atoms are the ideal systems to test experimentally these last corrections.

ii) Study of the corrections due to the proton finite size. We wish to reach sufficient precision in the measurements to be able to infer from the data significant informations about the proton form factor as seen by the muon.

iii) Test of μ-e universality, or more generally search for anomalous μ-P interactions.

iv) Experimental study of $(\mu p)^*$ atom formation and the ensuing cascade at different values of the hydrogen gas target pressure [3].

v) Extension of the above studies to the (μD) system.

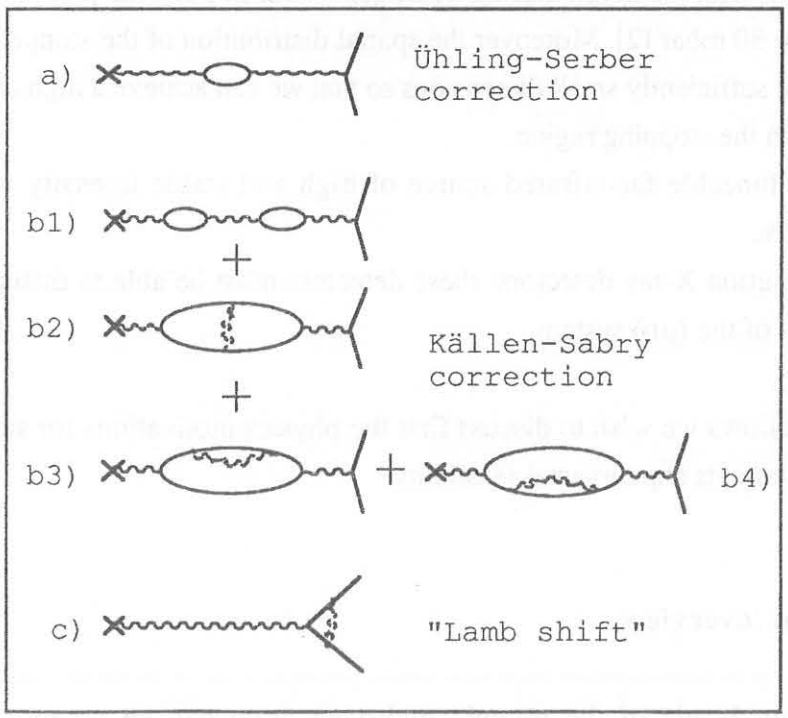

Figure 1: The lowest QED radiative corrections.
a) and b) vacuum polarization contributions; c) vertex correction.

To clarify point "i" it is especially important to review briefly the state of the art.

We recall that the values of the fine-structure constant α determined from condensed-matter physics (and independently of any QED corrections) are

from quantum Hall effect [4]:

$$\alpha_{QHE}^{-1} = 137.0359979\ (32) \qquad (1)$$

from AC Josephson effect [5]:

$$\alpha_{acJ}^{-1} = 137.0359770\ (77) \qquad (2)$$

The difference between these two values is approximately 3 standard deviations, a fairly large discrepancy if one recalls that both values should be free of "theoretical error". It has been argued [6] that the theoretical bases of the two determinations are not too clear and the theoretical consistency of the two methods has never been proved.
Obviously this discrepancy is crucial in all those cases in which the quantity measured depends very strongly on the value of α.

Let us now look at the results of the "g-2" experiments [7] as a source of the QED tests.

The electron anomaly $a_e = \frac{g-2}{2}$ can be computed theoretically as an expansion in terms of α:

$$a_e^{th} = c_1(\alpha/m) + c_2(\alpha/m)^2 + c_3(\alpha/m)^3 + c_4(\alpha/m)^4 + \ldots\delta_{ae} \qquad (3)$$

where $c_1, c_2, c_3, c_4, \delta_{ae}$ are quantities calculated using QED: using for α the value (1) one gets [6]

$$a_e^{th\ (QHE)} = 1.1596521400\ (53)\ (41)\ (271)\ 10^{-12} \qquad (4)$$

Using (2) would lead instead to a value $a_e^{th\ (acJ)} \approx 1.159651910\ 10^{-12}$. This difference shows that the experimental values [7]

$$a_{e+}^{exp} = 1.596521884\ (43)\ 10^{-12}$$
$$a_{e-}^{exp} = 1.596521879\ (43)\ 10^{-12} \qquad (5)$$

favour the value from the Quantum Hall effect rather than the one from AC Josephson effect.

Since the relative vacuum polarization correction to a_e^{th} is about 100 p.p.m. and the α theoretical determination discrepancy is 0.2 p.p.m. one sees that these measurements provide a test of this QED contribution at a level 2.0 10^{-3}.

Since a_e is so critically dependent on α equation (5) should rather be used to define α in the framework of QED; in fact assuming QED it is possible to derive the most precise value of α to date:

$$\alpha_{g\text{-}2}^{-1} = 137.03599222\ (94) \qquad (6)$$

$\alpha_{g\text{-}2}^{-1}$ is an order of magnitude more accurate than α_{QHE}^{-1} and α_{acJ}^{-1}.

In conclusion to test QED vacuum polarization contributions an experiment that is less dependent on the value of α is absolutely needed.

We turn now to the $(2S_{1/2}\text{-}2P_{1/2})$ Lamb shift results for ordinary hydrogen as a QED test :

The latest experimental results are [8]

$$\Delta E_{L.S.}^{exp} = 1057.845\ (9)\ MHz$$
$$\Delta E_{L.S.}^{exp} = 1057.851\ (2)\ MHz \qquad (7)$$

and these can be compared with the theoretical expectations:

$$\Delta E_{L.S.}^{th} = 1057.853\ (13)\ MHz \text{ for a proton rms radius} = 0.805\ (11)\ fm \qquad (8)$$

$$\Delta E_{L.S.}^{th} = 1057.871\ (13)\ MHz \text{ for a proton rms radius} = 0.862\ (11)\ fm \qquad (9)$$

Comparing (7), (8) and (9) and remembering that the QED contribution to (8) or (9) is $\approx 2.7\ 10^{-2}$ [6] one sees that the test of this term, due to the uncertainty of the proton rms radius, is at a level $1\ 10^{-3}$.

Of course assuming QED to be valid values (8) and (9) can be used to deduce the proton rms radius as seen by the electron. Thus one obtains [9]

$$(\text{proton rms radius})^e = 0.785 \pm 0.007\ fm$$

The agreement with (8) is barely acceptable, while is in contradiction with (9)

This experiment is indeed less dependent on α value as far as the QED vacuum polarization contributions test is concerned, however unfortunately it depends on the important empirical parameter that is the proton rms radius.

In table 1 we summarize the present experimental status of the QED vacuum polarization tests.

Now to support the main motivation of proposal R9206-1 presented at the P.S.I [1], a few comments are necessary:

a) It is interesting to see that today, the QED vacuum polarization corrections are checked to a level about 10^{-3}. The situation is almost the same as we had at the Zurich conference in 1978 [10] where a similar discussion was held. Since then the experimental accuracies in the Lamb shift and g-2 experiments have improved by more than an order of magnitude.

b) Given the reasons of the limitation in the QED vacuum polarization tests it is clear that accurate measurement on the elementary muonic system $(\mu p)^*$ can lead to a significant improvement and push the measurement accuracy above the 10^{-3} level.

In fact ,

- the dependence on α of the energy level differences is sufficiently weak that one is allowed to do QED vacuum polarization contribution tests beyond 10^{-3};
- choosing transitions that do not involve S levels one can avoid corrections due to the proton rms radius;
- at low pressure in the H_2 gas target there are certainly no electron screening corrections for the neutral $(\mu p)^*$ system

Table 1

exp.	momentum transfer (KeV/c)	limited by	QED v.p. test	quantity derived assuming QED
a_e	500	value of α	$2\ 10^{-3}$	α_{g-2}
$\Delta E_{L.S.}$	2	proton form factor	$1\ 10^{-3}$	proton rms radius = 0.785± 0.007 fm
$(2s - 2p)_{\mu He}$	370	nuclear form factor	$1.7\ 10^{-3}$	He rms radius = 1.673 ± 0.003 fm
$(3d_{5/2} - 2p_{3/2})$ in $^{28}Si\mu^-$ and $^{24}Mg\mu^-$	1000	electr. screening	$0.95\ 10^{-3}$	----------

In the final part of this paper we will show how the planned experiment might lead to an improved test of the QED vacuum polarization terms at a level of $(1 \div 2)\ 10^{-4}$. Such an improvement is possible and it can be done only at the PSI where muon beams that fulfil some of the necessary conditions for such an experiment already exist.

We will finish this section by looking more in detail at the energy levels for $n \leq 4$ for the (μp) system and at the lifetimes of the different levels.

The width Γ of the resonance will depend on the lifetimes of the levels involved: since we wish to reach a precision of $(2 \div 1)\ 10^{-4}$ in locating the resonances we think that the most appropriate transitions to look at are:

	line	$\Gamma/\Delta E$
1.	4S-4P	$4.2\ 10^{-4}$
2.	4P-4D	$4.3\ 10^{-3}$
3.	3P-3D	$5.3\ 10^{-3}$

Transitions (2) and (3) are particularly suitable for a QED vacuum polarization test since no proton rms radius corrections are needed, whereas transition (1) is suitable to extract information about the (proton rms radius)$^{\mu}$.

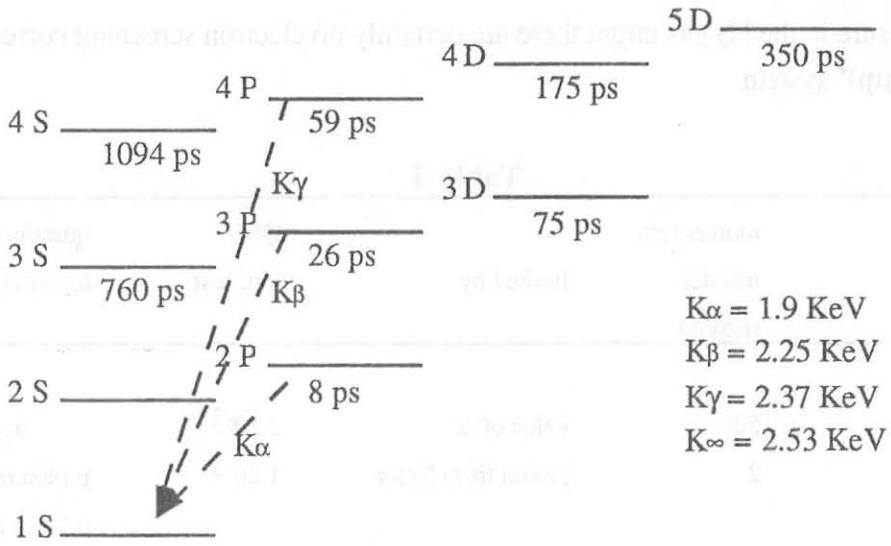

Figure 2: K lines and lifetimes of different levels for the (μp) system

If we turn again to figure 2 we may also note that each of the transitions schematically indicated actually represents many lines due to hyperfine sublevels.

Table 2 lists various energy level differences calculated from first order perturbation theory at the 1-2% level. Table 3 shows how the total energy is shared among the various contributions.

Table 2: The 4P-4D, 3P-3D and 4S-4P calculated energy differences for the various sublevels, arranged in order of increasing frequency (no vertex or finite size correction).

transition	hν	frequency	wavelength
$4P^{5}_{3/2} - 4D^{3}_{3/2}$	2.284 meV	552.2 GHz	543.275 μm
$4P^{5}_{3/2} - 4D^{5}_{3/2}$	2.566 meV	620.5 GHz	483.506 μm
$4P^{5}_{3/2} - 4D^{5}_{5/2}$	2.705 meV	654.1 GHz	458.676 μm
$4P^{3}_{3/2} - 4D^{3}_{3/2}$	2.754 meV	666.0 GHz	450.467 μm
$4P^{5}_{3/2} - 4D^{7}_{5/2}$	2.886 meV	697.9 GHz	429.837 μm
$4P^{3}_{3/2} - 4D^{5}_{3/2}$	3.037 meV	734.2 GHz	408.587 μm
$4P^{3}_{3/2} - 4D^{5}_{5/2}$	3.175 meV	767.8 GHz	390.714 μm
$4P^{3}_{1/2} - 4D^{3}_{3/2}$	3.218 meV	778.1 GHz	385.546 μm
$4P^{3}_{1/2} - 4D^{5}_{3/2}$	3.500 meV	846.4 GHz	354.451 μm
$4P^{1}_{1/2} - 4D^{3}_{3/2}$	4.394 meV	1063. GHz	282.342 μm
$3P^{5}_{3/2} - 3D^{3}_{3/2}$	5.307 meV	1283. GHz	233.803 μm
$3P^{5}_{3/2} - 3D^{5}_{3/2}$	5.976 meV	1445. GHz	207.621 μm
$3P^{5}_{3/2} - 3D^{5}_{5/2}$	6.305 meV	1525. GHz	196.779 μm
$3P^{3}_{3/2} - 3D^{3}_{3/2}$	6.422 meV	1553. GHz	193.198 μm
$3P^{5}_{3/2} - 3D^{7}_{5/2}$	6.735 meV	1629. GHz	184.210 μm
$3P^{3}_{3/2} - 3D^{5}_{3/2}$	7.091 meV	1715. GHz	174.966 μm
$3P^{3}_{3/2} - 3D^{5}_{5/2}$	7.42 meV	1794. GHz	167.203 μm
$3P^{3}_{1/2} - 3D^{3}_{3/2}$	7.521 meV	1819. GHz	164.960 μm
$3P^{3}_{1/2} - 3D^{5}_{3/2}$	8.190 meV	1980. GHz	151.482 μm
$3P^{1}_{1/2} - 3D^{3}_{3/2}$	10.31 meV	2493. GHz	120.346 μm
$4S^{3}_{1/2} - 4P^{1}_{1/2}$	25.89 meV	6261. GHz	47.9146 μm
$4S^{3}_{1/2} - 4P^{3}_{1/2}$	27.07 meV	6546. GHz	45.8326 μm
$4S^{3}_{1/2} - 4P^{3}_{3/2}$	27.53 meV	6658. GHz	45.0606 μm
$4S^{3}_{1/2} - 4P^{5}_{3/2}$	28.00 meV	6771. GHz	44.3035 μm
$4S^{1}_{1/2} - 4P^{1}_{1/2}$	29.42 meV	7114. GHz	42.1679 μm
$4S^{1}_{1/2} - 4P^{3}_{1/2}$	30.60 meV	7399. GHz	40.5469 μm
$4S^{1}_{1/2} - 4P^{3}_{3/2}$	31.06 meV	7511. GHz	39.9416 μm

As it will be clarified later we plan to start the experimental program [1] measuring with accuracy the lines:

$$\Delta_3 = 3D_{5/2}{}^7 - 3P_{3/2}{}^5 , \qquad (10)$$

$$\Delta_4 = 4D_{5/2}{}^7 - 4P_{3/2}{}^5 .$$

As far as the measurements of the 4S - 4P line and the study of (μD) atom are concerned these should be a further step in the future program.

Table 3: the main contributions to the 3P-3D energy differences

Transition	FS	HFS	Ühling	Källen	Total
$3P\ {}^5_{3/2} - 3D\ {}^3_{3/2}$	0. meV	0.8365 meV	-6.103 meV	-0.03975 meV	-5.307 meV
$3P\ {}^5_{3/2} - 3D\ {}^5_{3/2}$	0. meV	0.1673 meV	-6.103 meV	-0.03975 meV	-5.976 meV
$3P\ {}^5_{3/2} - 3D\ {}^5_{5/2}$	-0.8311 meV	0.6692 meV	-6.103 meV	-0.03975 meV	-6.305 meV
$3P\ {}^3_{3/2} - 3D\ {}^3_{3/2}$	0. meV	-0.2788 meV	-6.103 meV	-0.03975 meV	-6.422 meV
$3P\ {}^5_{3/2} - 3D\ {}^7_{5/2}$	-0.8311 meV	0.239 meV	-6.103 meV	-0.03975 meV	-6.735 meV
$3P\ {}^3_{3/2} - 3D\ {}^5_{3/2}$	0. meV	-0.948 meV	-6.103 meV	-0.03975 meV	-7.091 meV
$3P\ {}^3_{3/2} - 3D\ {}^5_{5/2}$	-0.8311 meV	-0.4461 meV	-6.103 meV	-0.03975 meV	-7.42 meV
$3P\ {}^3_{1/2} - 3D\ {}^3_{3/2}$	-2.493 meV	1.115 meV	-6.103 meV	-0.03975 meV	-7.521 meV
$3P\ {}^3_{1/2} - 3D\ {}^5_{3/2}$	-2.493 meV	0.4461 meV	-6.103 meV	-0.03975 meV	-8.19 meV
$3P\ {}^1_{1/2} - 3D\ {}^3_{3/2}$	-2.493 meV	-1.673 meV	-6.103 meV	-0.03975 meV	-10.31 meV

3. Requirements for the experimental apparatus.

When a μ^- is stopped in the H_2 gas target cavity it is captured by a proton and forms an atom with high n (n≈14), which subsequently cascades electromagnetically to the ground level. The natural transition probabilities combined with the statistical nature of the cascade process, yield well-defined intensities for the K_α, K_β, etc. lines at each gas pressure.

The cavity is also filled with FIR radiation from the tuneable source: when the frequency of this radiation has the right value to excite a transition between levels (like 3D -> 3P), the cascade process is changed and the relative intensities of the K lines also change.
We have already listed the most important parts of the apparatus that are necessary to implement this experimental program, and now we discuss in more detail points (2) and (3).

3.1 The beam, the target and the detector. As far as the low energy μ^- beam is concerned, the PSI accelerator complex has beams with momentum p less or equal to 30 MeV/c (πE1, πE5) and these beams are adequate when equipped with a high voltage separator to eliminate the electron contamination.

The x-ray detectors will be provided both by the Neuchatel group (commercial CCD's that have already been successfully tested in other measurements [11]) and by the Trieste group (silicon drift chambers, which are still at the research stage and have improved performances [12]).

As target chamber we plan to use "Cyclotron Trap" developed by L. Simons and collaborators [13]. In this target the incoming muon is tagged by a thin scintillator, and then it spirals to the centre of the trap as it loses energy in the rarefied H_2 gas that fills it. Eventually the muons stop in the centre of the trap: it has been shown that the muon stop distribution is a cigar-shaped gaussian distribution with a radius of 1 cm and with a length of 4 cm. This allows one to have a high energy density electromagnetic field overlapping the muon stop distribution and contained inside a Fabry-Perot resonant cavity.

Moreover a sufficiently low H_2 pressure can be used to stop the negative muons in the target so that we can minimize (especially in the case of the Δ_3 line) the statistical population of the 3P level. This is important since the deexcitation of this level is a main source of constant background. Fig. 3 shows the expected populations of the 3D and 3P levels versus pressure [14]: clearly the low pressure is quite convenient since the 3D level is highly populated while the 3P is not. We plan to work in the range 10-30 mbar. Similar considerations apply to the n = 4 populations.

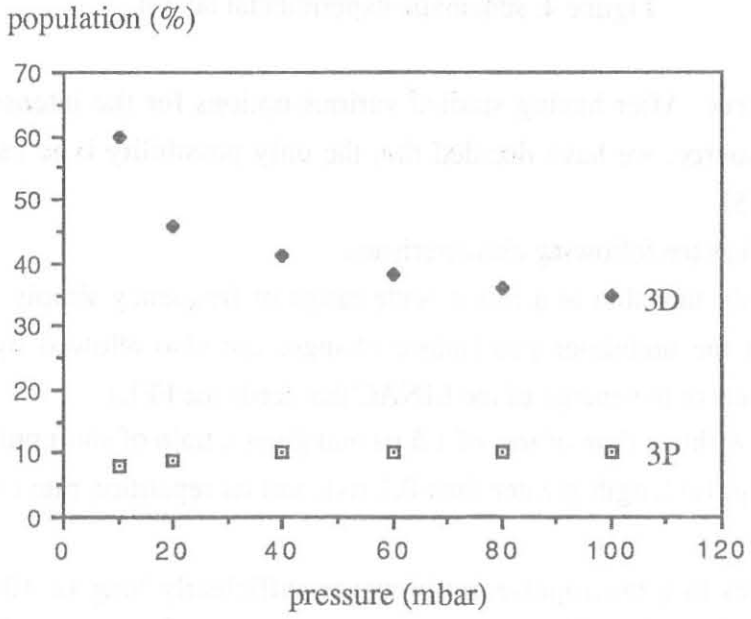

Figure 3: Expected populations of the 3D and 3P levels vs. pressure [14]

Using the tagging scintillator as a start signal it has been found experimentally that the stopping time distribution has a FWHM of about 300 nsec. We can also tune the pressure and the magnetic field in the trap so that the muons stop in the centre of the trap approximately 1.5 μsec after the start signal.

Thus the muons stop in a temporal window that is 300 nsec wide and appears 1.5 μsec after the scintillator signal: this allows a synchronization with the tuneable laser source (which has a discharge time approximately 1.5 μsec long).
Figure 4 shows how these parts might be arranged.

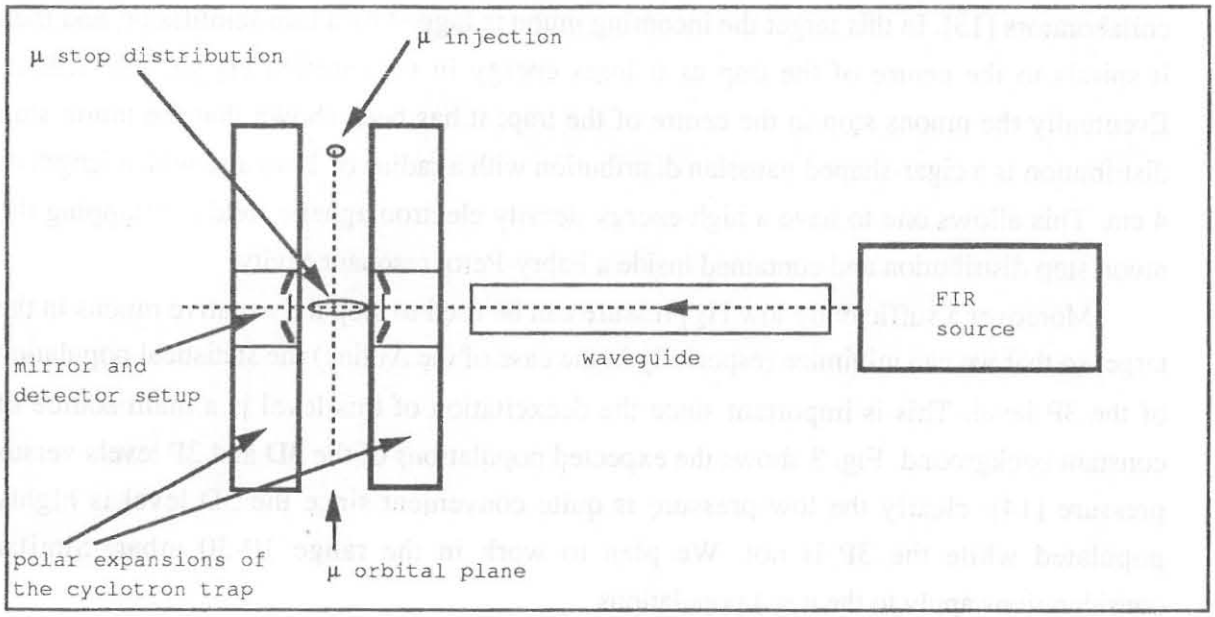

Figure 4: schematic experimental layout

3.2 The FIR source. After having studied various options for the intense and tuneable electromagnetic source, we have decided that the only possibility is to use a FEL (Free Electron Laser) [15].

This source has the following characteristics:

1. it is continuously tuneable in a rather wide range of frequency simply by varying the magnetic field or the undulator gap (major changes are also allowed by changing the undulator parameters or the energy of the LINAC that feeds the FEL)

2. it is triggerable within a time of less of 1.5 μs and gives a train of short pulses of radiation (for a total macropulse length greater than 0.5 μs), and its repetition rate can reach 100 to 200 Hz.

3. The short pulses in a macropulse are however sufficiently long (≥ 100 ps) to give a sufficiently small linewidth. The lines (Δ_3 and Δ_4) that we wish to study have a width of about 5 10^{-3}, and the FEL has approximately the same linewidth.

4. The peak energy in each pulse is sufficiently high to induce an acceptable number of transitions above the background due to spontaneous deexcitation.

The FEL is presently under study at the ENEA laboratories (Frascati); table 4 gives an approximate set of FEL parameters.

Eventually we expect to have a $\Delta\nu/\nu \approx 0.4$ % and a 60 kW average macropulse power.

Table 4: FEL parameters (3P - 3D line operation)

Electron energy	9 MeV
Radio Frequency	3 GHz
Macropulse duration	≥ 0.5 μs
Micropulse duration (after stretcher)	≥ 100 ps
Undulator period	5 cm
Number of periods	30
Output wavelength	160 μm - 320 μm
Radiation macropulse power	20 kW
Beam waist	≤ 2 mm
Repetition rate	100 - 200 Hz

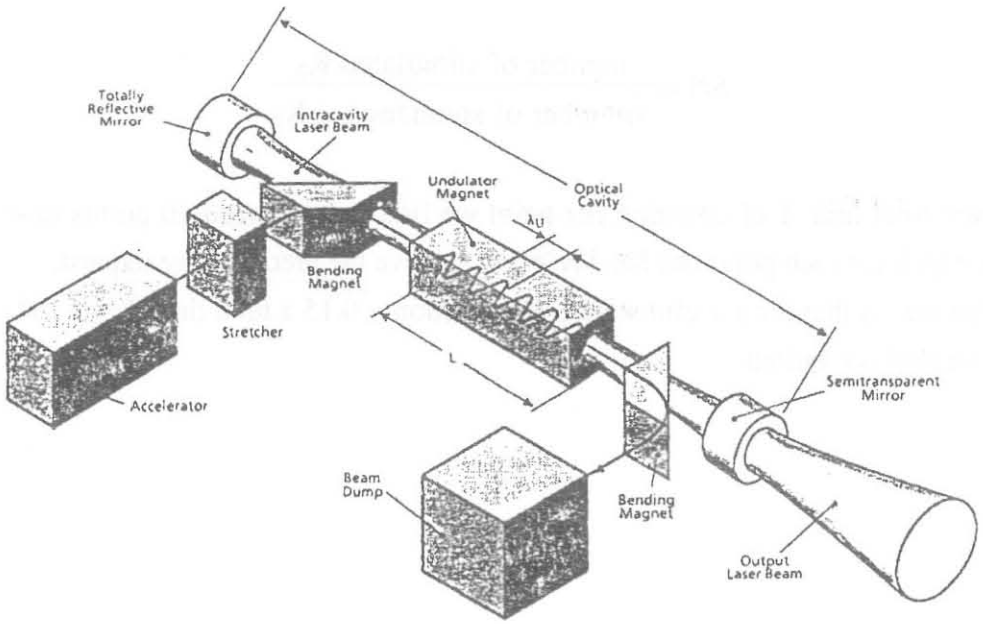

Figure 5: FEL layout

4. Rates

An accurate evaluation of the transition probability requires the exact quantum mechanical treatment of the two levels involved (this is given in P.Hauser's contribution to this conference). However (as shown by P.Hauser) a straightforward application of the Fermi golden rule is sufficient for a first evaluation of the transition probabilities, which are then given by the expression:

$$T_{a->b}\,(\omega = \omega_{res}) = \frac{16\pi^2\alpha I_0}{h}\, f\, \frac{1}{[\Gamma_a\,(\Gamma_a + \Gamma_b)]}\, R \qquad (11)$$

where $f \approx 0.7$ is a factor that takes into account the finite laser pulse length of about 100 ps, $\Gamma_a = 1/\tau_{3D}$, $\Gamma_b = 1/\tau_{3P}$ are the natural level linewidths and I_0 is the average intensity of radiation in the cavity that overlaps the muon stop distribution (≈ 6.7 kW/cm^2). R is the average number of reflections of the laser beam in the cavity (≈ 100).

Therefore if the 3D initial state population is $\approx 50\%$ of the stopped muons and the 3P population is $\approx 8\%$ of the stopped muons, and noting that the statistical population of the $3D_{5/2}$[7] level is 35% of the total 3D population, one obtains for the ratio $Q_{\beta,\alpha}$

$$Q_{\beta,\alpha} = \frac{\text{stimulated K}\beta\text{ intensity}}{\text{spontaneous K}\beta\text{ intensity}}$$

a value of $\approx 2\%$.

So tuning the laser around the resonance value of the Δ_3 transition one should see a peak 2% higher than the spontaneous emission background. Calling

$$SN = \frac{\text{number of stimulated K}\beta}{\sqrt{\text{number of spontaneous K}\beta}}$$

for a given total time T of counting per point we find that we need 10 points (around the peak) in which for each point one has $SN \geq 5$ to achieve the precision we request.

This means that for a useful solid angle fraction ≈ 0.15 a total time $T \approx 2\ 10^6$ sec (i.e. about 5 weeks) is required.

5. References

[1] P.S.I. Proposal R-9206-1, "Spectroscopy of muonic hydrogen" (Dec. 1991)

[2] H.Anderhub et al., Phys.Lett. **143B** (1984) 65

[3] A. Di Giacomo, Nucl.Phys. **B11** (1969) 411. See also E.Borie and G.A.Rinker, Rev.Mod.Phys. **54** (1982) 67

[4] M.E.Cage et al., IEEE Trans.Instrum.Meas. **38** (1989) 233

[5] E.R.Williams, IEEE Trans.Instrum.Meas. **38** (1989) 284

[6] T.Kinoshita and D.R.Yennie: "High Precision Tests of Quantum Electrodynamics - An Overview", in T.Kinoshita (ed.) "Quantum Electrodynamics",World Scientific (Singapore, 1990)

[7] R.S.Van Dyck et al., Phys.Rev.Lett. **59** (1987) 26

[8] E.Zavattini: "Transitions in muonic helium", in G.F.Bassani,M.Inguscio and T.Hänsch (eds.) "The Hydrogen Atom", Springer-Verlag (New York, 1989)

[9] Yu.Sokolov: in G.F.Bassani,M.Inguscio and T.Hänsch (eds.) "The Hydrogen Atom", Springer-Verlag (New York, 1989)

[10] E.Zavattini "Quantum Electrodynamics Tests in Muonic Systems", in the Proceedings of the 7th International Conference on High-Energy Physics, M.Locher editor, Birkhäuser-Verlag (Basel, 1978)

[11] See, e.g. J-P.Egger et al.: "Progress in X-ray detection", to be published in Physics World

[12] See, e.g. E.Gatti and P.Rehak, Nucl.Instr.and Meth. **225** (1984) 608, and P.Rehak et al., Nucl.Instr. and Meth. **A248** (1986) 367

[13] L.M.Simons, Phys.Scrip. **T22** (1988) 90

[14] Courtesy of L.M.Simons, from a cascade code developed by E.Borie and M.Leon, Phys.Rev. **A21** (1980) 1460

[15] See e.g. P.Sprangle and T.Coffey, Phys.Today March 1984, p.44 for a general overview of FEL's and other high-power sources. V.L.Granatstein et al., IEEE Trans.on Microwave Th.and Techn., **MTT-22** (1974) 1000 is a "historical" source on radiation from relativistic electron beams. A "sample" of the activity of the ENEA group is given e.g. in Nucl.Instr.and Meth. **A272** (1988) 132.